AIChE

Nonstationary Fault Detection and Diagnosis for Multimode Processes

Jialin Liu
Dept. of Information Management, Fortune Institute of Technology, Kaohsiung, Taiwan, Republic of China

Ding-Sou Chen
Dept. of New Materials Research and Development, China Steel Corporation, Kaohsiung, Taiwan, Republic of China

DOI 10.1002/aic.11999
Published online August 31, 2009 in Wiley InterScience (www.interscience.wiley.com)

Fault isolation based on data-driven approaches usually assume the abnormal event data will be formed into a new operating region, measuring the differences between normal and faulty states to identify the faulty variables. In practice, operators intervene in processes when they are aware of abnormalities occurring. The process behavior is nonstationary, whereas the operators are trying to bring it back to normal states. Therefore, the faulty variables have to be located in the first place when the process leaves its normal operating regions. For an industrial process, multiple normal operations are common. On the basis of the assumption that the operating data follow a Gaussian distribution within an operating region, the Gaussian mixture model is employed to extract a series of operating modes from the historical process data. The local statistic T^2 *and its normalized contribution chart have been derived for detecting abnormalities early and isolating faulty variables in this article.* © 2009 American Institute of Chemical Engineers *AIChE J,* 56: 207–219, 2010

Keywords: process monitoring, principal component analysis, Gaussian mixture model, kernel density estimation, contribution charts

Introduction

The requirement for improving process efficiency and avoiding unexpected shutdowns in the process industry has led to increased research activity in fault detection and diagnosis (FDD). Venkatasubramanian et al.[1–3] broadly categorized the methods of FDD into three classes, namely, (1) quantitative model-based methods, (2) qualitative model representations, and (3) process history-based methods. Most of the model-based approaches rely on state-space equations and the model parameters estimated from input–output data. However, the state variables and model structures may be different due to the changes of control strategies for committing the demands of different product grades in a multimode process. It is hard to distinguish whether the residuals of model-based approaches come from the model structure assumptions or the measurement errors. The qualitative method is usually developed by capturing process personnel knowledge with cause–effect relations, such as: if-then-else rules, signed digraphs (SDG), and fault tree analysis. As the models are developed based on subjective cognition, they may conflict from different field experts' understandings of the process. In contrast to model-based approaches where the process knowledge is needed before building the model, data-driven methods model the process with historical data, with the process knowledge involved in the postanalysis stage. The data-driven methods can be broadly classified as linear and nonlinear approaches. Statistical tools, such as, principal component analysis (PCA), partial least squares (PLS), …etc., are the linear approaches to extract feature information from process data. Artificial neural networks (ANN) are the most popular counterparts. As these kinds of

Correspondence concerning this article should be addressed to J. Liu at jialin@center.fotech.edu.tw

approaches are usually time invariant, the model may be invalid due to the time-varying nature of real processes. In practice, adapting models with new event data should be a concern in this category method.

In the absence of prior process knowledge or rich operating experience, applying statistical tools onto historical process data, and then discussing the analysis results with field experts is more preferable for FDD than a model-based approach. Yoon and MacGregor[4] comprehensively compared model-based and statistical methods for FDD. PCA[5] is the most popular multivariate statistical tool applied to process monitoring. To project normal operating data onto the subspace expanded by PCs, control limits of statistic Q and T^2 are defined. The former measures Euclidean distance from an observation to the subspace, the latter measures Mahalanobis distance from a score vector to the origin of the subspace. The contribution charts[6,7] of Q and/or T^2 are investigated to isolate the faulty variables when the control limits of Q and/or T^2 are violated.

PLS[8] is another popular statistical tool for monitoring a process with two block data, such as process on-line measurements and quality data from the laboratory. MacGregor et al.[9] and Kourti and MacGregor,[10] respectively applied PLS to monitor a low-density polyethylene process. The faulty variables were isolated successfully by exploring the contribution charts. Canonical variate analysis (CVA) was also applied to two block data. The most significant difference with PLS is CVA with two sets of mutual orthogonal least latent variables (LVs) that maximize the cross covariance of two block data. The two sets of LVs are not correlated so that CVA lacks prediction capability unlike PLS. Russell et al.[11] compared the fault detection performance of CVA, PCA, and dynamic PCA[12] (DPCA). They reported the CVA is more sensitive than the others, so its control limits need to be adjusted to achieve robustness. Martin and Morris[13] derived a T^2-like statistic and its control limits by using kernel density estimation[14] (KDE) from the score vectors to release the assumption that data onto the PCA subspace have to be a normal distribution. Chen et al.[15] extracted the probability density function (PDF) with, respectively, confidence limits by using KDE for monitoring processes with multiple operating conditions. Chen et al.[16] synthesized the T^2 and Q statistics into one Shewhart chart of the joint PDF, which is estimated with kernel density estimation. They reported that the sensitivity of the monitoring charts to the abnormalities is improved.

Bayesian classification method is a popular tool for unsupervised pattern recognition.[17] Banerjee et al.,[18] Deshpande and Patwardhan[19] respectively used the method to classify multiple linear operating regions, in which each local model was derived using a model-based approach. The multiple piecewise linear models were then applied to a nonlinear model predictive control[18] and an online fault diagnosis,[19] respectively. Wang and McGreavy[20] applied Bayesian automatic classification (AutoClass) developed by NASA to cluster data from a FCCU into classes corresponding to various operating modes. Yu and Qin[21] used the Figueiredo-Jain (F-J) algorithm to determine the cluster parameters of Bayesian classification. In their approach, a fault detection index was derived based on Mahalanobis distance and the posterior probability of each cluster; however, faulty variables were not isolated when the index exceeded its control limits. Mehranbod et al.[22,23] derived fault detection and identification indices based on probabilistic information of Bayesian belief networks (BNN) to detect and identify bias, drift, and noise in sensor readings for a polymerization reactor at steady-state conditions and transition states. In their approach, a mathematical model of the process or fault-free process data is prerequisite to describe the correlation between each parent–child pair of sensor nodes of the multisensor BBN. It can be expected that the networks will be complicated for a complex chemical process with massive measurements.

Kruger and Dimitriadis[24] integrated PLS with statistical local approach[25] to isolate faulty variables with variable biases during process upsets. The approach is suitable for processes with single mode operating regions due to PLS being a linear statistical tool. Raich and Çinar[26,27] built several PCA models using normal and abnormal process data. The faulty variables are isolated by measuring the differences between models, including statistical distances and angle measures. He et al.[28] used k-means clustering to classify historical data into different groups. The pairwise Fisher discriminant analysis (FDA) was then applied to normal data and each class of fault data to find fault directions that were used to generate contribution plots for isolating faulty variables. Liu and Chen[29] used Bayesian classification to extract multiple operating regions from historical data. A fault identification index was derived based on the differences between normal and abnormal cluster centers and covariances. These fault isolation methods are based on the assumption that abnormal events eventually went into a new steady state operation whose data formed a cluster or a model. In practice, operators intervene in the process and try to bring it back to normal operations when abnormal situations occur. There is no chance to form an abnormal class for this situation. Even if an abnormal class has been formed, the variables separating normal and abnormal classes may not be the faulty variables inducing the abnormal event. One purpose of this work is to derive normalized contribution charts of local statistic T^2 for isolating faulty variables in the first place when an abnormal event is detected. It should be noted that the proposed approach is not to derive a method to model nonstationary behavior of a process, such as: time series method,[30] cointegration testing method.[31] Instead of that, the proposed method systematically extracts a series of operating modes from historical process data whereas statistically defines control limits for each mode. As long as online data leave from the known operating modes, the event can be detected promptly; no matter the process behavior of the abnormal event is stationary or nonstationary.

Another purpose of this work is to modify the Bayesian classification algorithm, in which the Gaussian mixture model is employed to represent multiple operating regions based on the assumption of data variation following a Gaussian distribution within a quasi-steady-state operation. Generally, the maximum likelihood (ML) method is used to estimate the parameters of the Gaussian mixture model, the means and covariances of each density function and the priori probabilities. The solution of the ML problem, usually known as the expectation-maximization (EM) procedure,

suffers three well-known difficulties.[32] First, there are many local maxima that cause inconsistent solutions from different initial conditions for local maximum seeking algorithms. Second, the numbers of clusters have to be predefined. Lastly, outliers and transition data are inevitable in a real plant dataset. They will affect the parameters of Gaussian density functions and cause instability in the convergence of the parameter optimization. The proposed approach provides a systematic method to estimate a reasonable initial condition for EM iteration by using KDE. A local statistic T^2 for each cluster has been derived for trimming outliers and transition data during the EM procedure. The reminder of the article is organized as follows. The basic theory of Bayesian classification, PCA, and KDE are presented in basic theory section. Proposed approach section summarizes the overall strategy for monitoring a process with multiple operating regions. The quadruple-tank laboratory process and a real process problem from an industrial plant are given in illustrative example section demonstrating the effectiveness of the proposed approach. Finally, some conclusions are given in industrial application section.

Basic Theory

Bayesian classification

In this subsection, the Bayesian classification method is briefly described. The details can be found in reference.[17] The priori probabilities that c classes exist are P_j, $j = 1,\ldots,c$. Given the conditional probability density functions of $\mathbf{x}_i$ in class j $p(\mathbf{x}_i|j;\boldsymbol{\theta})$:

$$p(\mathbf{x}_i|j;\boldsymbol{\theta}) = \frac{p(\mathbf{x}_i, j)}{P_j} \tag{1}$$

where $p(\mathbf{x}_i, j)$ is the joint probability of the $\mathbf{x}_i$ and the jth class, and $\boldsymbol{\theta}$ is the parameter vector of the conditional probability density function. The posteriori probabilities can be found from Bayes rule.

$$P(j|\mathbf{x}_i;\boldsymbol{\theta},\mathbf{P}) = \frac{p(\mathbf{x}_i|j;\boldsymbol{\theta})P_j}{\sum_{k=1}^{c} p(\mathbf{x}_i|k;\boldsymbol{\theta})P_k} \tag{2}$$

Here, $\mathbf{P} = (P_1, P_2,\ldots,P_c)$ is the priori probability vector. If the parameters of the conditional probability density functions and priori probabilities are known, the posteriori probabilities can be calculated from Eq. 2. Those parameters can be iterated from the Expectation-Maximization (EM) algorithm. If a multivariate Gaussian distribution function is used as a conditional probability function:

$$p(\mathbf{x}_i|j;\boldsymbol{\mu},\Sigma) = \frac{1}{(2\pi)^{n/2}\left|\Sigma_j\right|^{1/2}} \exp\left(-\frac{1}{2}\left(\mathbf{x}_i-\boldsymbol{\mu}_j\right)\Sigma_j^{-1}\left(\mathbf{x}_i-\boldsymbol{\mu}_j\right)^{\mathrm{T}}\right) \tag{3}$$

with $\boldsymbol{\mu}_j$ and Σ_j being the mean vector and covariance matrix of class j. The parameters $\boldsymbol{\theta}$ are given by $\boldsymbol{\mu} = [\boldsymbol{\mu}_1,\ldots,\boldsymbol{\mu}_c]$ and $\Sigma = [\Sigma_1,\ldots,\Sigma_c]$. The above optimization problem can be solved by the following iterative algorithm:

E-Step:
Calculate the posteriori probabilities as follows:

$$P(j|\mathbf{x}_i;\boldsymbol{\mu}(t),\Sigma(t)) = \frac{p(\mathbf{x}_i|j;\boldsymbol{\mu}(t),\Sigma(t))P_j(t)}{\sum_{k=1}^{c} p(\mathbf{x}_i|k;\boldsymbol{\mu}(t),\Sigma(t))P_k(t)} \tag{4}$$

M-Step:
Compute the next estimated parameters by:

$$\boldsymbol{\mu}_j(t+1) = \frac{\sum_{k=1}^{m} P(j|\mathbf{x}_k;\boldsymbol{\mu}(t),\Sigma(t))\mathbf{x}_k}{\sum_{k=1}^{m} P(j|\mathbf{x}_k;\boldsymbol{\mu}(t),\Sigma(t))}, \quad j = 1\ldots c \tag{5}$$

$$\Sigma_j(t+1) = \frac{\sum_{k=1}^{m} P(j|\mathbf{x}_k;\boldsymbol{\mu}(t),\Sigma(t))\left(\mathbf{x}_k-\boldsymbol{\mu}_j(t)\right)^T\left(\mathbf{x}_k-\boldsymbol{\mu}_j(t)\right)}{\sum_{k=1}^{m} P(j|\mathbf{x}_k;\boldsymbol{\mu}(t),\Sigma(t))} \tag{6}$$

$$P_j(t+1) = \frac{1}{m}\sum_{i=1}^{m} P(j|\mathbf{x}_i;\boldsymbol{\mu}(t),\Sigma(t)) \tag{7}$$

The solution of maximum log-likelihood function is found by repeating E and M steps until every parameter has converged to within a tolerance criterion ε.

Given a system with d variables and c clusters, the number of iterated parameters is $c(d + d(d + 1)/2) + (c - 1)$ for Eqs. 5–7. In general $c \geq 2$, the number of iterated parameters is proportional to the square of the number of variables. Thus, the computing burden will be significantly relieved, if the variable dimensions are reduced without a loss of data feature. Multiple run[33] is the common approach to determine the number of clusters by evaluating information indices, such as: Akaike's information criterion (AIC), Bayesian information criterion (BIC), normalized entropy criterion (NEC), …etc. Obviously, a high computational load is needed for this approach. Even if the number of cluster is set, the unstable convergence of EM still occurs because the random initializations trap the iterated parameters by local maximum. Therefore, predetermining the correct number of clusters and their proper locations can reduce the computational load and cope with the unstable convergence.

Principal component analysis

Consider the data matrix $\mathbf{X} \in R^{m\times n}$ with m rows of observations and n columns of variables. Each column is normalized to zero mean and unit variance. The eigenvectors ($\mathbf{P}$) of the covariance matrix can be obtained from the normalized dataset. The data matrix $\mathbf{X}$ can be decomposed as:

$$\mathbf{X} = \sum_{i=1}^{K} \mathbf{t}_i\mathbf{p}_i^{\mathrm{T}} + \sum_{i=K+1}^{n} \mathbf{t}_i\mathbf{p}_i^{\mathrm{T}} = \hat{\mathbf{X}} + \mathbf{E} \tag{8}$$

where $\mathbf{t}_i$ is the ith score vector; $\hat{\mathbf{X}}$ being the projection of the data matrix $\mathbf{X}$ onto the subspace formed by the first K eigenvectors and $\mathbf{E}$ being the remainder of $\mathbf{X}$ that is orthogonal to the subspace.

The statistic Q is defined to examine whether the new data belong to the PCA subspace.

$$Q = \mathbf{x}\left(\mathbf{I} - \mathbf{P}_K\mathbf{P}_K^T\right)\mathbf{x}^{\mathrm{T}} \tag{9}$$

The loading vectors $\mathbf{P}_K \in R^{m\times K}$ are the first K terms of eigenvectors of covariance matrix. The confidence limits of Q can be found in Jackson.[5] Another measure of the difference between new data and the PCA subspace is the statistic T^2.

$$T^2 = \mathbf{x}\mathbf{P}_K\Lambda^{-1}\mathbf{P}_K^{\mathrm{T}}\mathbf{x}^{\mathrm{T}} \tag{10}$$

The diagonal matrix Λ is first K terms of eigenvalues, where $\Lambda = \mathrm{diag}[\lambda_1\ \lambda_2,\ldots,\lambda_K]$. However, the control limits of T^2 are derived based on the assumption that the scores on the PCA subspace can be described by a multivariate normal distribution function. For a multimode process, the assumption is invalid, and the local T^2 statistics are provided in the later section to detect process variation of systematic parts.

A new contribution chart of T^2 has been provided as follows:

$$T^2 = \mathbf{t}_K\Lambda^{-1}\mathbf{t}_K^{\mathrm{T}} = \tilde{\mathbf{t}}_K\tilde{\mathbf{t}}_K^{\mathrm{T}} = \tilde{\mathbf{t}}_K\mathbf{P}_K^{\mathrm{T}}\mathbf{P}_K\tilde{\mathbf{t}}_K^{\mathrm{T}} = \tilde{\mathbf{x}}\tilde{\mathbf{x}}^{\mathrm{T}} = \sum_{i=1}^{n}\tilde{x}_i^2 \tag{11}$$

where $\mathbf{t}_K$ are the first K term scores, $\tilde{\mathbf{t}}_K = \mathbf{t}_K\Lambda^{-0.5}$ are the scores weighted by corresponding eigenvalues, and $\mathbf{P}_K^{\mathrm{T}}\mathbf{P}_K = \mathbf{I}_K$ is used. To plot each $\tilde{x}_i$ for n original variables, their control limits can be obtained from a normal distribution[34] since the data variation follows a multivariate Gaussian distribution within a normal operating condition. It should be noted that the contribution chart of $\tilde{x}_i$ is preserved with its sign indicating whether the faulty variables are higher or lower than their normal values. For a gradually developing abnormality, the data variations are still within the PCA subspace in the first place and the T^2 statistics are capable of detecting the early upsets. Therefore, it is useful to investigate the contribution chart of T^2 chronologically to locate the faulty variables in the first place when the Q is still under its control limits.

Kernel density estimation

Kernel density estimation (KDE) is a nonparameter statistical tool to construct a density function from the observed data. In this subsection, KDE is briefly described. The details can be found in reference.[14] Given the sampled data $\mathbf{X} \in R^{m\times d}$ with m observations in d-dimensional space, the density function can be estimated with kernel function K and a smoothing parameter h, also known as window width or bandwidth:

$$\hat{f}(\mathbf{x}) = \frac{1}{mh^d}\sum_{i=1}^{m}K\left(\frac{\mathbf{x}-\mathbf{X}_i}{h}\right) \tag{12}$$

In practice, the kernel function is chosen with a multivariate normal density function:

$$K(\mathbf{z}) = (2\pi)^{-d/2}\exp\left(-\mathbf{z}^{\mathrm{T}}\mathbf{z}/2\right) \tag{13}$$

However, the form of the kernel function is not very important, as long as it satisfies:

$$\int_{-\infty}^{\infty}K(\mathbf{z})\,\mathrm{d}\mathbf{z} = 1 \tag{14}$$

In this article, the adaptive kernel approach[14] is used to determine the smoothing parameter. The approach allows the smoothing parameter to vary from one observation to another. The local bandwidths corresponding to the various observations are initially estimated by a pilot density function. After that, the adaptive kernel estimate is generated by the local bandwidths. The strategy is given as follows:

1. Find a pilot estimate $\tilde{f}(\mathbf{x})$ that satisfies $\tilde{f}(\mathbf{X}_i) > 0$ for $i = 1,\ldots,m$. As the adaptive kernel estimate is insensitive to the pilot density, the initial window width h can be derived from the density function, which is composed of a series of multivariate normal distributions, with continuous second derivatives.

$$h = [4/(d+2)]^{1/(d+4)}m^{-1/(d+4)} \tag{15}$$

2. Define the local bandwidth factor λ_i for each observation by

$$\lambda_i \equiv \left[\tilde{f}(\mathbf{X}_i)/g\right]^{-0.5} \tag{16}$$

where g is the geometric mean of the $\tilde{f}(\mathbf{x})$, i.e., $\log g = m^{-1}\sum_{i=1}^{m}\log\tilde{f}(\mathbf{X}_i)$.

3. The adaptive kernel estimate $\hat{f}(\mathbf{x})$ can be written as:

$$\hat{f}(\mathbf{x}) = m^{-1}\sum_{i=1}^{m}(\lambda_i h)^{-d}K\left[(\lambda_i h)^{-1}(\mathbf{x}-\mathbf{X}_i)\right] \tag{17}$$

It should be noted that one of the advantages of applying the adaptive kernel approach is that the smoothing parameter h is determined directly by Eqs. 15 and 16. Extra tuning parameters are not needed to estimate the density function of scores on the PCA subspace.

Proposed Approach

Modified Bayes classifier

In this subsection, the modified Bayes classifier has been proposed. A PCA subspace is built for the training dataset. The density function of the scores on the PCA subspace is obtained through KDE with the compressed data. The local maxima of the density function can be reached by using a nonsmooth function optimizer with several initial guesses. Once the numbers of clusters and the initial values have been determined, the EM procedure is performed to obtain cluster parameters. However, the outliers and transition data stretch cluster covariances into an infeasible region. The local T^2 statistic for each cluster is provided to trim outliers and transition data after the converging of each EM.

After converging the EM steps, perform singular value decomposition (SVD) on each cluster covariance.

$$\Sigma_i = \mathbf{U}_i \Lambda_i \mathbf{U}_i^{\mathrm{T}}, \quad i = 1, ..., c \tag{18}$$

where Λ_i is a diagonal matrix with eigenvalues of the ith cluster covariance, and $\mathbf{U}_i$ is a full matrix with corresponding eigenvectors. The local T^2 statistic for the ith cluster can be obtained from the Mahalanobis distance to the cluster center:

$$T_i^2 = (\mathbf{t} - \boldsymbol{\mu}_i)\Sigma_i^{-1}(\mathbf{t} - \boldsymbol{\mu}_i)^{\mathrm{T}} = (\mathbf{t} - \boldsymbol{\mu}_i)\mathbf{U}_i \Lambda_i^{-1} \mathbf{U}_i^{\mathrm{T}}(\mathbf{t} - \boldsymbol{\mu}_i)^{\mathrm{T}} \tag{19}$$

where $\mathbf{t}$ is a score vector on the PCA subspace, and $\boldsymbol{\mu}_i$ is the ith cluster center. Since the conditional probability density is a normal distribution, the confidence limits of the ith cluster can be defined as:

$$T_{i,\alpha}^2 = \frac{K(m_i - 1)}{m_i - K} F_{K,m_i - 1,\alpha} \tag{20}$$

where m_i is the number of observations belonging to the ith cluster, K is the dimension of the subspace, and $F_{K,m_i-1,\alpha}$ is an F distribution with degrees of freedom K and $m_i - 1$ within $(1 - \alpha)$ confidence limits. Thus, the proposed algorithm is as follows:

1. PCA is applied to reduce variable dimensions and the number of retained PCs is determined by cross validation without loss of data feature.

2. The density function of the scores is estimated by KDE from Eq. 17. The local maxima of the density functions are used as initial conditions of the EM procedure.

3. Repeat the EM steps, from Eqs. 4–7, until converging to a stable solution.

4. Evaluate the local T^2 for each cluster from Eq. 19 with its control limits from Eq. 20. Outliers and transition data can be recognized and discarded if all local T^2 of a sample are out of the corresponding control limits. Go back to step 3, until all retained data are within the respective local T^2 control limits.

The proposed approach takes advantage of the well-known difficulties of EM; that is the iterated parameters trapped by local optimum. Therefore, a stable solution will be obtained as long as the number of clusters and their centers are estimated properly. To ensure the covariances literally reflect the data variations during steady states, outliers and transition data have to be trimmed gradually after each EM convergence. It should be noted that the tuning parameters of the proposed approach are the confidence limits of local T^2, which are intuitive and with statistical meaning.

Nonstationary fault isolation

The proposed local T^2 statistics are not only used to trim outliers at the data clustering stage, but also to monitor the systematic variations for a multimode process. Thus, the contribution charts of local T^2 are derived in this subsection. Once statistic Q of the new data is within the control limits but the T^2 exceeds its limits, the PCA model still is capable of explaining the data. At that moment, the contribution charts of local T^2 reveal very useful information for diagnosing root causes of process faults, since the PCA is still valid whereas the abnormality develops initially. Equation 18 indicates that $\mathbf{U}_i$ contains the principal directions of the ith cluster covariance on the PCA subspace. Therefore, the weightings of the original variables to the principal directions are $\mathbf{P}_K\mathbf{U}_i$, and the relations between original variables and principal directions of the ith cluster can be revealed by plotting each column vector of $\mathbf{P}_K\mathbf{U}_i$ versus the original variables, analogizing to the loading plots of PCA. The contrition charts of local T^2 can be obtained by rewriting Eq. 19:

$$T_i^2 = \tilde{\mathbf{t}}_i \tilde{\mathbf{t}}_i^{\mathrm{T}} = \tilde{\mathbf{t}}_i \mathbf{U}_i^{\mathrm{T}} \mathbf{P}_K^{\mathrm{T}} \mathbf{P}_K \mathbf{U}_i \tilde{\mathbf{t}}_i^{\mathrm{T}} = \tilde{\mathbf{x}}_i \tilde{\mathbf{x}}_i^{\mathrm{T}} = \sum_{j=1}^{n} \tilde{x}_{ij}^2 \tag{21}$$

in which $\tilde{\mathbf{t}}_i = (\mathbf{t} - \boldsymbol{\mu}_i)\mathbf{U}_i \Lambda_i^{-0.5}$, $\mathbf{P}_K^{\mathrm{T}}\mathbf{P}_K = \mathbf{I}_K$, and $\mathbf{U}_i^{\mathrm{T}}\mathbf{U}_i = \mathbf{I}$ are used. The faulty variables can be isolated by plotting each normalized contribution plot of $\tilde{x}_{ij}$ for n original variables, when the ith local T^2 exceeds its control limits. As the data variation follows a multivariate Gaussian distribution within a quasi-steady-state operation, the control limits for each $\tilde{x}_{ij}$ can be obtained from a normal distribution. In this article, all contribution charts have been normalized with 99% confidence limits, and its sign has been preserved.

Illustrative Example

Quadruple-tank laboratory process

The quadruple-tank process was developed by Johansson[35] as a multivariable laboratory process with an adjustable zero. The process consists of four interconnected water tanks, two pumps, and associated valves. A nonlinear model is derived based on mass balances and Bernoulli's law as follows:

$$\frac{dh_1}{dt} = -\frac{a_1}{A_1}\sqrt{2gh_1} + \frac{a_3}{A_1}\sqrt{2gh_3} + \frac{f_1}{A_1}, \quad f_1 = \gamma_1 k_1 v_1 \tag{22a}$$

$$\frac{dh_2}{dt} = -\frac{a_2}{A_2}\sqrt{2gh_2} + \frac{a_4}{A_2}\sqrt{2gh_4} + \frac{f_2}{A_2}, \quad f_2 = \gamma_2 k_2 v_2 \tag{22b}$$

$$\frac{dh_3}{dt} = -\frac{a_3}{A_3}\sqrt{2gh_3} + \frac{f_3}{A_3}, \quad f_3 = (1 - \gamma_2) k_2 v_2 \tag{22c}$$

$$\frac{dh_4}{dt} = -\frac{a_4}{A_4}\sqrt{2gh_4} + \frac{f_4}{A_4}, \quad f_4 = (1 - \gamma_1) k_1 v_1 \tag{22d}$$

where A_i is the cross section of the Tank i, a_i is the cross section of the outlet and h_i is the water level. The voltage applied to Pump i is v_i and the corresponding flow is $k_i v_i$. The flow to Tank 1 is $\gamma_1 k_1 v_1$ and the flow to Tank 4 is $(1-\gamma_1)k_1 v_1$ and similarly for Tank 2 and Tank 3. The acceleration of gravity is denoted as g. The quadruple-tank process has been studied at two operating modes. The parameter values and the initial water levels are listed in Table 1.

The normal operating data with two modes were generated by using Eqs. 22a–d with respective parameters listed in Table 1. Tank levels h_1–h_4 and flow rates f_1–f_4 were observed per 10 sec, in which the sampling values were corrupted by Gaussian white noise with zero mean and standard deviation of 0.05. For each mode, 100 observations were collected. PCA was applied to the normal operating data and 2 PCs were retained by using cross-validation. The PCA model captured about 99% of the total variance. The two scores with control limits have been shown in Figure 1, in which the dash line and solid line respectively are 95 and 99% confidences. It is obvious that the scores do not

Table 1. Simulation Parameters for the Quadruple-Tank Process with Two Operating Modes

Parameter	Unit	Mode 1	Mode 2
A_1, A_3	cm^2	28	
A_2, A_4	cm^2	32	
a_1, a_3	cm^2	0.071	
a_2, a_4	cm^2	0.057	
g	cm/s^2	981	
h_1, h_2	cm	12.4, 12.7	12.6, 13.0
h_3, h_4	cm	1.8, 1.4	4.8, 4.9
v_1, v_2	V	3.00, 3.00	3.15, 3.15
k_1, k_2	cm^3/Vs	3.33, 3.35	3.14, 3.29
γ_1, γ_2		0.7, 0.6	0.43, 0.34

distribute following a multivariate Gaussian distribution. Therefore, a conventional T^2 statistic is inadequate to monitor a process with multiple operating modes. The density function of the scores was estimated by KDE without prior knowledge about the process. Several initial guesses were uniformly distributed over the density function, and the local maxima were located by using a nonsmooth function optimizer as Figure 2a shows. The local maxima of the density function were used as the initial conditions of EM iterations. In this example, since the transition data were not concerned, the clustering parameters were converged after rejecting two outliers in Figure 2b, in which the solid lines represent the 99% confidence limit for each local T^2 statistic and cluster C1 and C2 were labeled as operating regions of Mode 1 and Mode 2. Comparing Figure 2b with Figure 1, the local T^2 is more suitable to monitor a multimode process than conventional statistic T^2.

Two abnormal situations, stationary and nonstationary faults, were studied in this work. For each one, 100 normal operating data were generated by using Eqs. 22a–d with parameters of Mode 1 before inducing an abnormal event. After that, 100 abnormal event data were generated. The first case is from He et al.[28] They assumed that there was a small hole at the bottom of Tank 1 with the cross section $a_{\text{leak}} = 0.005\ cm^2$. The mass balance equation for Tank 1 is rewritten as:

$$\frac{dh_1}{dt} = -\frac{a_1}{A_1}\sqrt{2gh_1} + \frac{a_3}{A_1}\sqrt{2gh_3} + \frac{f_1}{A_1} - \frac{a_{leak}}{A_1}\sqrt{2gh_1},\ f_1 = \gamma_1 k_1 v_1 \tag{23}$$

The other balance equations do not change. In this case, the process variables soon reached to a new steady state, so it is called a stationary fault. In the second case it was assumed that the cross section of Tank 3 was gradually blocked as:

$$a_3 = 0.071\left(1 - \frac{t - 1000}{2000}\right), \quad t > 1000 \tag{24}$$

In the end, the cross section of Tank 3 was the half of the original size. The mass balance equations were same as the

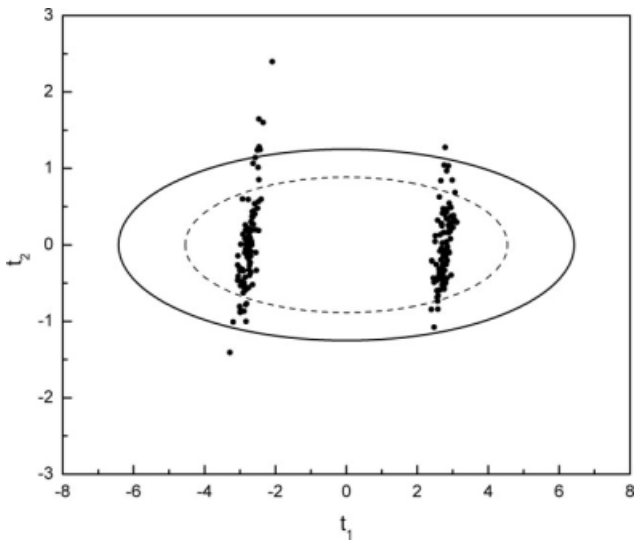

Figure 1. The score plot of the normal operating data with two modes.

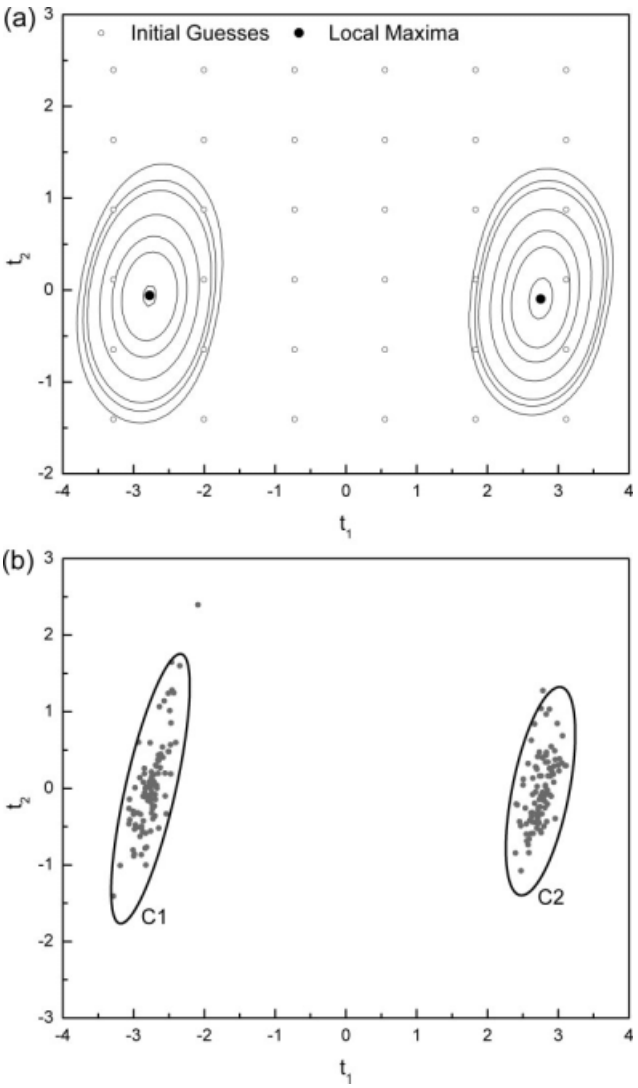

Figure 2. Data clustering procedure, (a) contour plot of density function, initial guesses (○), and local maxima (●), (b) convergence of EM iterations.

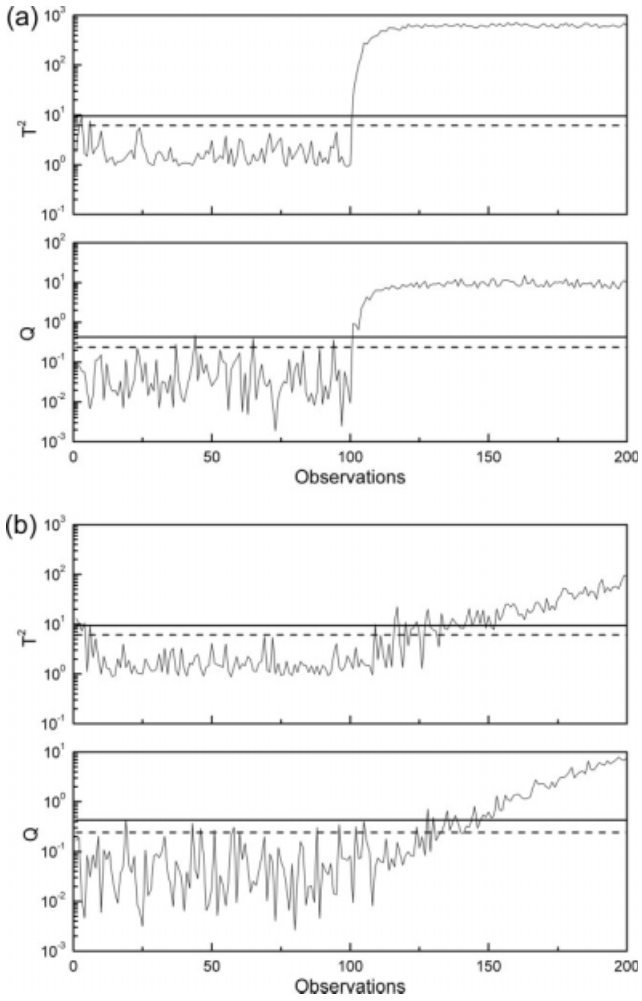

Figure 3. The statistic Q and T^2 of PCA subspace built by normal operating data, (a) for the first case, (b) for the second case.

normal operating condition. The process behavior was nonstationary during the period of generating the second case data. Figure 3 shows the conventional PCA detected both abnormal situations. For the first case, the statistic Q and T^2 exceeded their control limits after the 100th observation and reached to stable values, as Figure 3a shows. On the contrary, the gradually developing fault could not be detected immediately after the 100th observation for the second case. The abnormality could be identified until the fault magnitude was built up. It should be noted that both statistics would not reach to stable values for a nonstationary fault in Figure 3b.

The PCA subspace has to be adapted when monitoring a time-varying process. The detailed strategies of monitoring a time-varying process with multiple operating states can be found in the previous work.[29] In this example, the subspace was individually updated by using the two case data for fair comparisons. After adapting the PCA subspaces, both case data were under the control limits, as Figure 4 shows. It demonstrates any recursive PCA model for monitoring time-varying processes would be misled by blindly updating, especially in a multimode process. The drawback can be eliminated by introducing local statistic T^2. The cluster parameters of two operating modes can be directly transferred to the updating subspaces.[29] The local statistic T^2 of the first case has been shown in Figure 5a, in which all data were far from C2, meanwhile the leading 100 data belonged to C1 and the rest of them were rejected by C1. Figure 5b shows all data of the second case also did not belong to C2, whereas the data slowly drifted away from C1 after the 100th sample. They were consistent with data generating manners for both cases.

The normalized contribution charts of the local statistic T^2 were built for cluster C1 in Figure 6. The variables labeled 1–8, respectively, are the measurements h_1–h_4 and f_1–f_4. Figure 6a shows the measurement h_1 was under its control limit since the 101th observation, from which the abnormal event was induced. In Figure 6b, the measurement h_3 firstly exceeded its upper control limit from the 116th sample. Subsequently, the measurement h_1 was lower than its control limit. It is consistent with the process behavior when the cross section of Tank 3 was gradually blocked. The fault directions by pairwise FDA[28] of the two cases have been shown in Figure 7. The fault direction of the first case

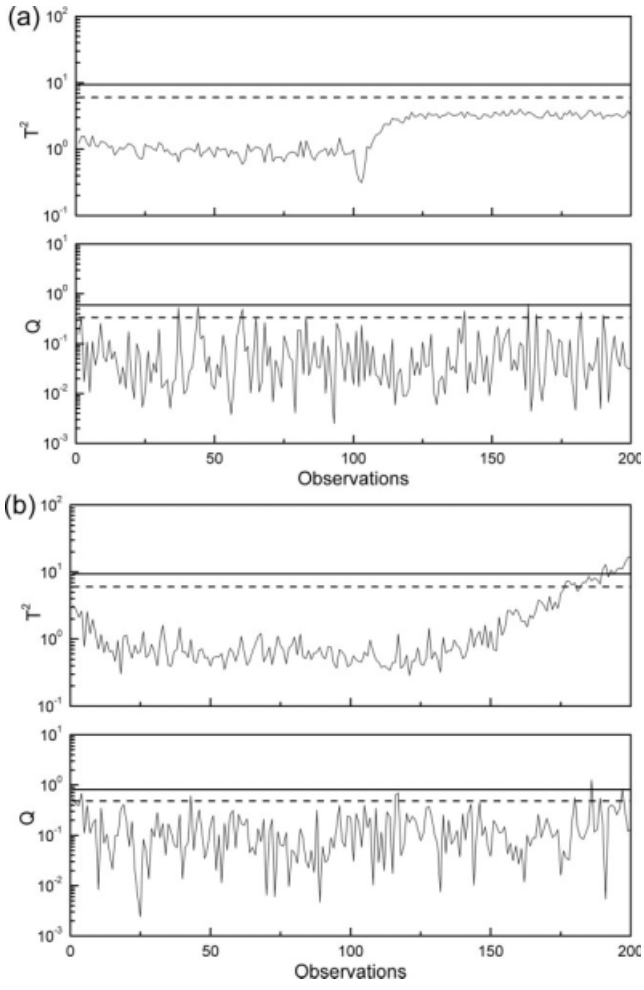

Figure 4. The statistic Q and T^2 of adapting PCA subspace, (a) with the first case data, (b) with the second case data.

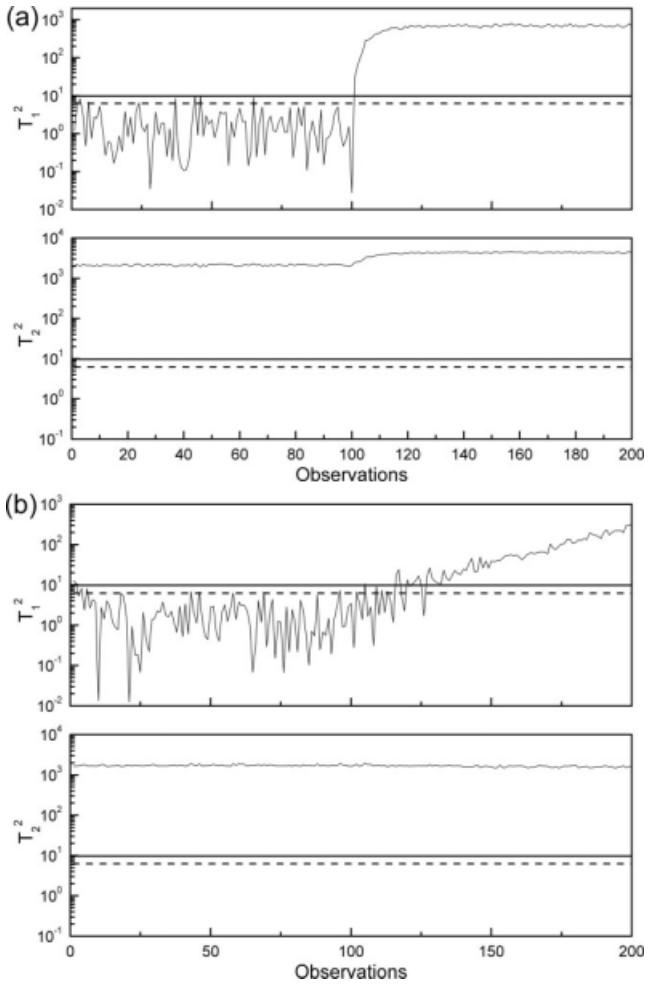

Figure 5. Local statistic T^2 of each mode, (a) for the first case, (b) for the second case.

indicates the faulty variable was h_1, as Figure 7a shows. It is consistent with what He et al.[28] reported. However, the faulty variable of the second case also was h_1, as Figure 7b shows. The level of Tank 3 should be higher than normal operating condition was not revealed by FDA. It is because the FDA found a suitable direction to separate two data clusters. The abnormal event data of the second case could not be grouped into a cluster due to its nonstationary behavior. Even the abnormal event data could be grouped into a cluster when the process reached into a new steady state. It is not guaranteed that the direction between two groups, which were normal and faulty states, indicated the *real* faulty variables in the first place.

Industrial application

China Steel Corporation (CSC) is an integrated steel maker, which produces steel from iron ore. In the production steps, the blast furnace and oxygen converter are the most important processes. Both processes are oxygen-intensive ones. To supply a high purity of oxygen, CSC runs several stand-alone oxygen plants. Essentially, it is an air separation process in the oxygen plant. The process input is air, coming from the atmosphere, and the products are oxygen, nitrogen, and argon. The compressed air was fed into the Pressurized Column through stream 1, as Figure 8 shows. Part of the N_2 product was drawn from the top of the Pressurized Column. Stream 3, which mostly consisted of O_2 and Ar, was used as a coolant of the condensers of Crude Argon Column 2 and the Pure Argon Column. It was then fed into the Low Pressure Column through stream 4 to withdraw the rest of the N_2 from the top of the Low Pressure Column. The O_2 and Ar would be separated by Crude Argon Column 1 and 2, and the Pure Argon Column. The Ar purity of stream 8 from the Crude Argon Column reached around 99%, and then was fed into the Pure Argon Column. The specification of product purity of Ar from the Pure Argon Column was 99.9999%. Figure 8 shows that the five distillation columns are highly integrated. Therefore, the operators often complained the process was too sensitive to be operated. When they were aware of abnormal situations from the measurements, it usually was too late to manipulate set points to bring the process back to normal operations. For example,

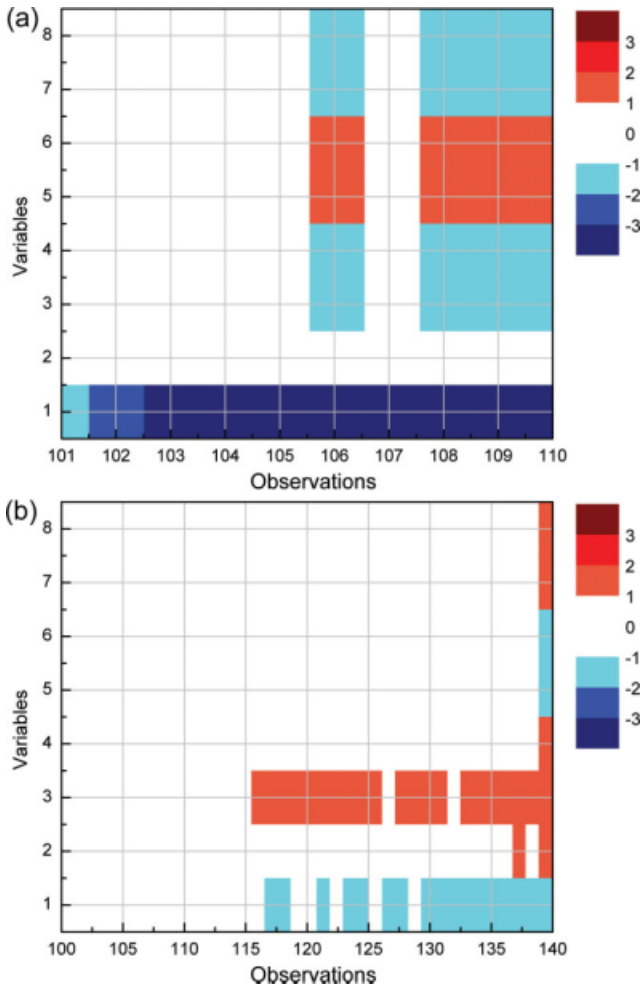

Figure 6. The normalized contribution plots of the local T^2, (a) for the first case, (b) for the second case.

[Color figure can be viewed in the online issue, which is available at www.interscience.wiley.com.]

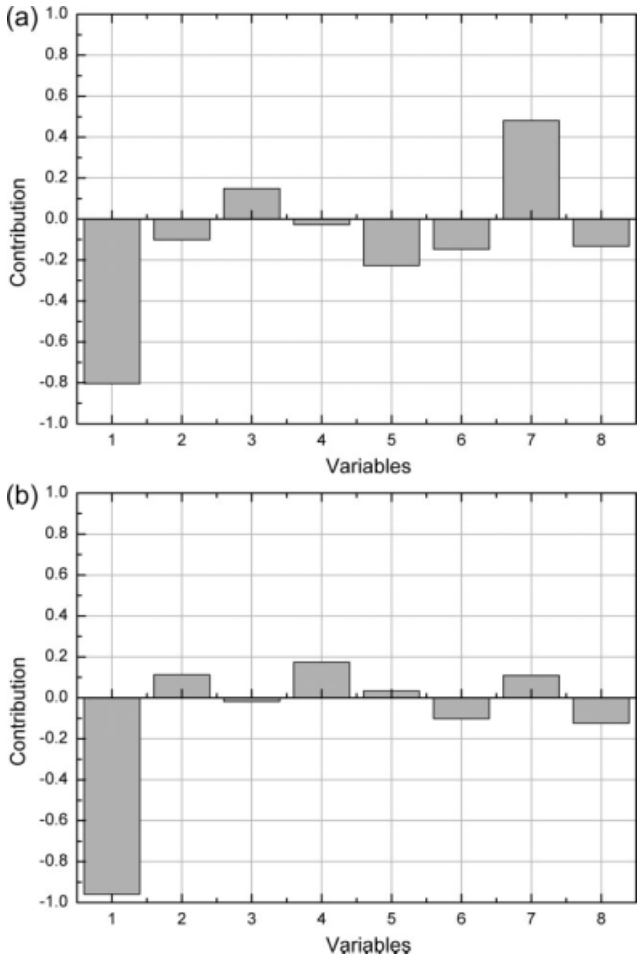

Figure 7. The fault direction from Fisher discriminant analysis, (a) for the first case, (b) for the second case.

when they found the feed flow of the Pure Argon Column, stream 8, highly fluctuated, the only thing they could do was to bypass the inlet, i.e., temporarily stop producing high purity Ar until the flowrate had settled down. The operators were frustrated by the abnormalities frequently emerging.

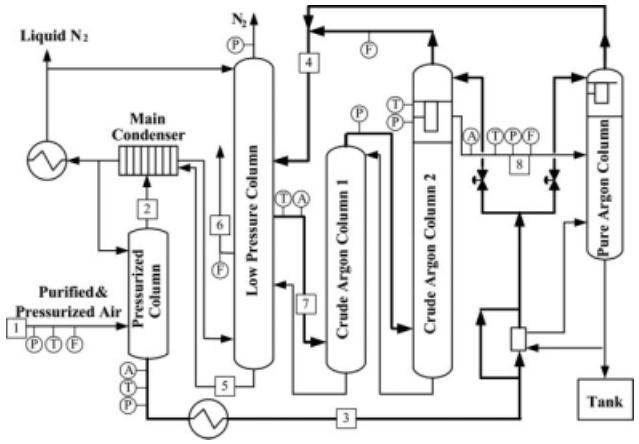

Figure 8. Air separation process flow diagram.

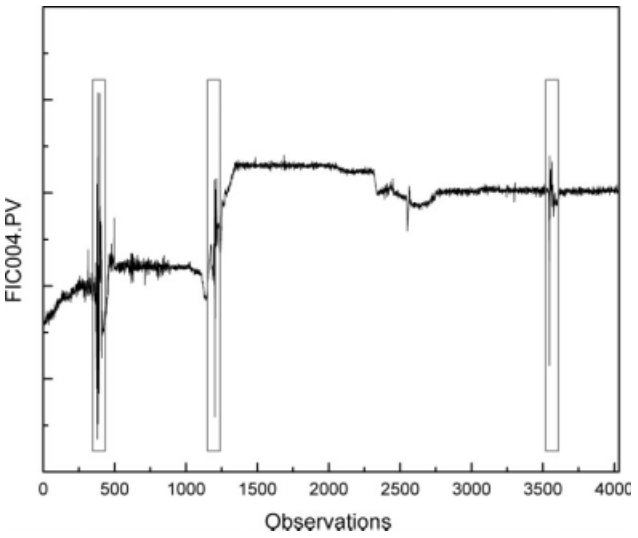

Figure 9. Feed flow of pure argon column highly fluctuated during abnormal situations.

Figure 9 shows the upsets happened three times during 2 weeks in which, the data were collected every 5 min. In the next 2 months, similar situations occurred eight times. They fervently need an early fault detection tool to prevent the upset. Furthermore, they wanted to realize what the root cause was and how to prevent it.

Figure 9 displays that the process behavior of abnormal events was nonstationary, so the approaches of measuring the differences between normal and faulty states were invalid for this case. The time frame of Figure 9 was investigated in this study, collecting the data of measured variables listed in Table 2 every 5 min. There were 4032 observations in the reference dataset. Among them were 3902 observations that could be explained by the PCA subspace, in which the captured variances were 87% with three PCs, within 99%

Table 2. Measured Variables for the Air Separation Process

No.	Variable	Description
1	FIC001.PV	Flowrate of stream 1
2	PIC001.PV	Pressure of stream 1
3	TI001.PV	Temperature of stream 1
4	AIC001.PV	O_2 concentration of stream 3
5	TIC002.PV	Temperature of stream 3
6	PIC002.PV	Pressure of stream 3
7	FIC002.PV	Flowrate of stream 6
8	AIC002.PV	O_2 concentration of stream 7
9	TIC003.PV	Temperature of stream 7
10	PIC003.PV	Pressure of top of low pressure column
11	PI004.PV	Pressure of top of crude argon column 1
12	FIC003.PV	Flowrate of top of crude argon column 2
13	TI004.PV	Temperature of stream 8
14	AIC003.PV	O_2 concentration of stream 8
15	FIC004.PV	Flowrate of stream 8
16	PIC005.PV	Pressure of stream 8
17	PI006.PV	Condenser pressure of crude argon column 2
18	TI005.PV	Condenser temperature of crude argon column 2

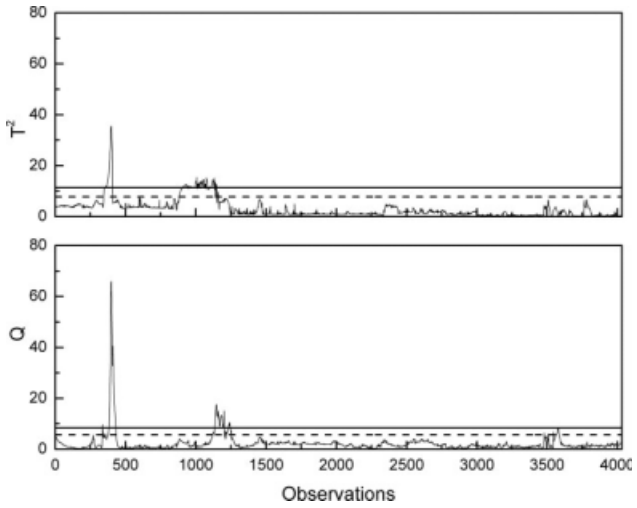

Figure 10. The statistic Q and T^2 for the reference dataset.

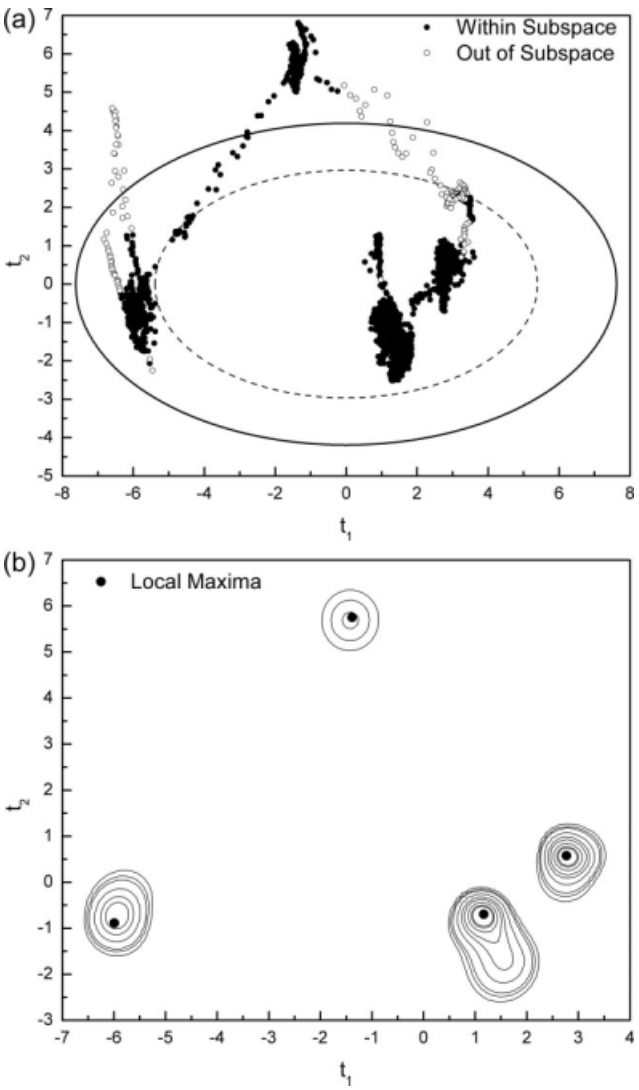

Figure 11. Project reference data on PCA subspace with the first two PCs, (a) the score plot and its control limits, (b) contour plot and local maxima.

confidence limits. The statistic Q and T^2 of the reference dataset have been shown in Figure 10. Compared with Figure 9, the first two upsets were captured by Q and T^2 and the third was missed. Projecting the reference data onto the PCA subspace, Figure 11a shows the first two scores. There were multiple operating modes in the reference dataset. The density function of scores was estimated by KDE and the contour plot of density function with local maxima has been shown in Figure 11b. The EM iteration was initialized using Figure 11b. Figure 12 compares the convergences of EM with and without transition data. It is obvious that the transition data would stretch the cluster covariances into infeasible operating regions. The results show the proposed data clustering method of being capable of rejecting outliers effectively.

The comparisons of high fluctuations of the Pure Argon Column inlets, the statistic Q, and the local T^2 have been shown in Figure 13. For the first two upsets, which could be detected by the Q charts, the local T^2 control limits had been violated before the Q exceeded its control limits, as Figures 13a and b show. The fault magnitude of the third upset was smaller than the first two so it could not be captured by the statistic Q. However, Figure 13c shows the local T^2 had violated its control limits at the 3505th sample, earlier than the inlet fluctuation, which began at the 3540th sample. Figure 13 demonstrates the effectiveness of early fault detection by the local T^2 charts for the multimode process. The normalized contribution charts of the local statistic T^2 have been shown in Figure 14. Figures 14a and b report a lot of faulty variables simultaneously for the first two upsets. Compared with Figure 14c only variables 7 and 9 are firstly reported for the third upset. Variable 7, FIC002.PV, was used to regulate variable 9, TIC003.PV. When the temperature of stream 7 was higher than its set point, the withdraw flowrate from the Low Pressure Column increased through stream 6. Before the third upset occurred, the

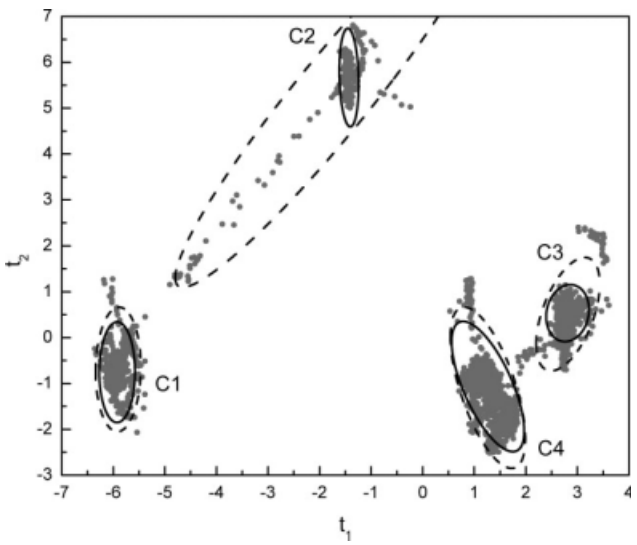

Figure 12. Clusters of the reference data within the subspace, where solid and dash lines, respectively, represent the transition data were trimmed or not.

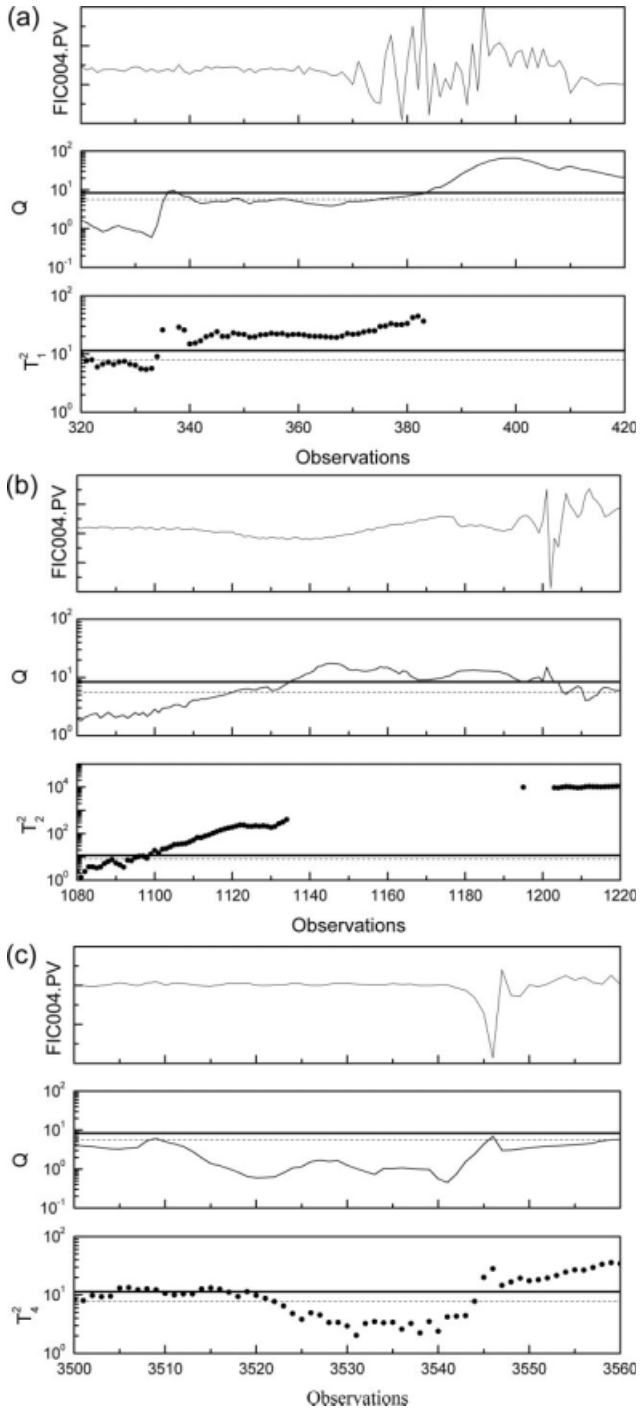

Figure 13. Comparisons of local T^2, statistic Q, and the feed flow of Pure Argon Column, (a) the first upset, (b) the second upset, and (c) the third upset in Figure 9.

TIC003.PV was higher than its set point so the FIC002.PV was increasing until the valve saturated, as Figure 15 shows. It explains why the FIC004.PV dramatically decreased around the 3545th sample in Figure 13c. However, this faulty scenario was not suitable for the first two upsets, since variables 7 and 9 were not reported in Figures 14a and b.

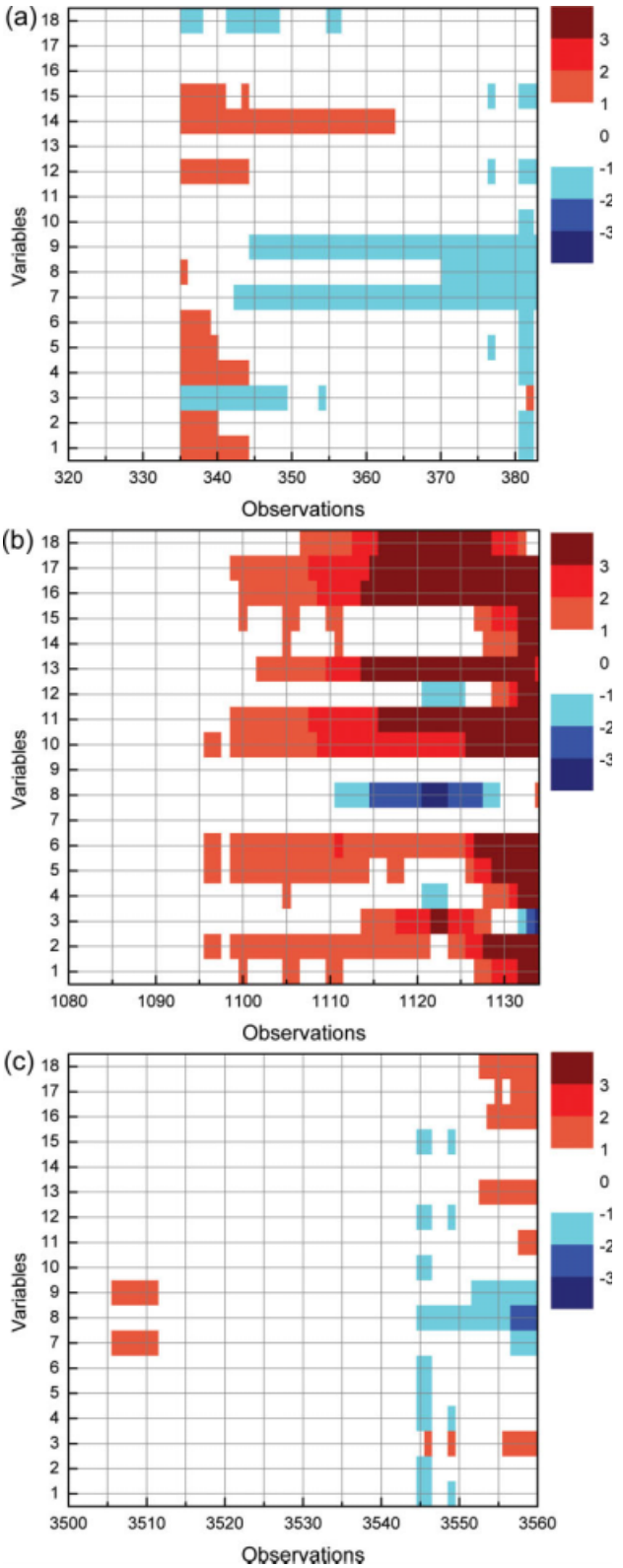

Figure 14. The normalized contribution plots of local T^2 statistic, (a) for cluster C1, (b) for cluster C2, and (c) for cluster C4.

[Color figure can be viewed in the online issue, which is available at www.interscience.wiley.com.]

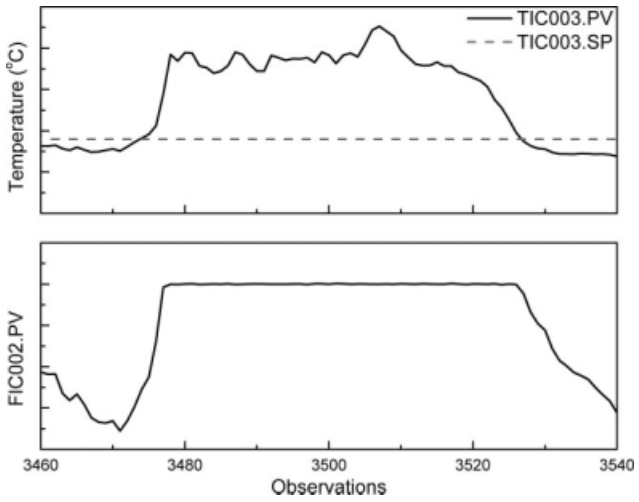

Figure 15. The trends of variable 7 (FIC002.PV) and 9 (TIC003.PV) before the third upset.

On further investigation of Figures 14a and b, one of the common contributions of T^2 is the variable 3 being too low and/or variable 2 being too high, i.e., the inlet temperature and pressure of the Pressurized Column. The phase diagram of the inlet operating condition has been shown in Figure 16. If the inlet temperature is too low and/or the pressure too high, which are from point A going into point B and/ or into point C in Figure 16, the inlet condition would go into two phases. In addition, Figure 8 shows that the separation process does not have any reboiler from the outsides; it has been insulated; known as Cold Box. The inlet energy of the Pressurized Column is the only heat source to vaporize the liquid in the columns in the Cold Box. If the inlet energy is not sufficient to support the liquid in the columns, then column dumping would occur. Figures 14a and b indicate that the first two upsets might be due to the inlet condition going into two phases. The inlet temperature of the reference dataset has been compared with the dew point and bubble point

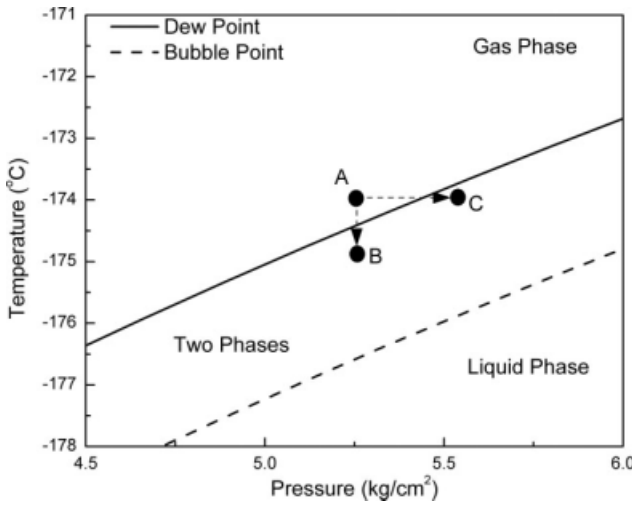

Figure 16. Phase diagram of the operating condition for the inlet of Cold Box.

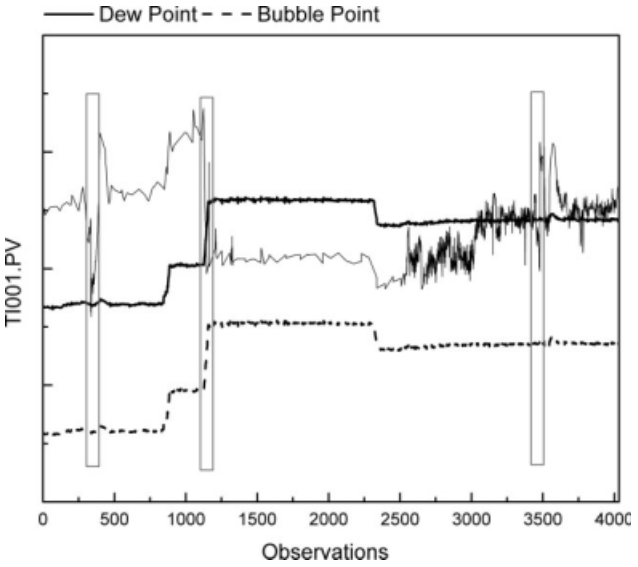

Figure 17. The inlet condition of the pressurized column while pure argon column inlet highly fluctuating.

of the inlet condition in Figure 17. It shows the inlet temperatures were lower than the dew points of the inlet condition before FIC004.PV began highly fluctuating. It can be concluded that the root cause of the Pure Argon Column inlet being highly fluctuating is due to the inlet energy of the Cold Box not being sufficient to support the liquid in the columns, and then inducing the Crude Argon Column to dump. For preventing similar abnormalities from reoccurring, a real-time dew point is calculated from the inlet pressure that has been provided to compare with the inlet temperature. The operators have been requested to keep the inlet temperature above the dew point that has been compiled into their standard operating procedure (SOP). Since then, the abnormal situation has disappeared.

Conclusion

In this article, a nonstationary fault detection and diagnosis for multimode processes has been dealt with. The contributions of this article are as follows:

1. Resolved the well-known difficulties of EM iterations by introducing KDE to locate the initial conditions of EM and deriving the local T^2 to trim outliers and transition data for each EM procedure. The former estimates the numbers of clusters and cluster centers effectively, and the latter ensures the cluster covariances literally reflect the data variations during steady-state operations. It should be noted that the tuning parameters of the proposed approach only are the confidence limits of the local T^2, which are intuitive and statistically reasonable.

2. The T^2 chart of conventional PCA is invalid for a multimode process. It should be replaced by the local T^2 charts for monitoring the systematic part of the PCA. However, the statistic Q is still valid for a multimode process, as long as the retained PCs are capable of capturing the systematic variations from the reference data.

3. The normalized contribution charts of local T^2 are derived are directly related to the measured variables. The faulty variables are located in the first place when the abnormal event occurs by analyzing the contribution chart chronologically. In addition, the normalized chart with sign indicates whether the faulty variables are higher or lower than the normal values.

The industrial application demonstrates the effectiveness of the proposed approach for a process with multiple operating conditions. The abnormal situation can be detected early by local T^2 charts, prolonging the response time for operators to bring the process back to normal states. The more promising advantage is to locate the faulty variables correctly by investigating the normalized contribution chart chronologically. It would be clearer to diagnose the root cause if the faulty variables were isolated precisely.

Acknowledgments

This work was supported by the National Science Council, Republic of China, under Grant NSC-97-2221-E-268-002, and by the China Steel Corporation.

Literature Cited

1. Venkatasubramanian V, Rengaswamy R, Yin K, Kavuri SN. A review of process fault detection and diagnosis. Part I: quantitative model-based methods. *Comput Chem Eng*. 2003;27:293–311.
2. Venkatasubramanian V, Rengaswamy R, Kavuri SN. A review of process fault detection and diagnosis. Part II: qualitative models and search strategies. *Comput Chem Eng*. 2003;27:313–326.
3. Venkatasubramanian V, Rengaswamy R, Kavuri SN, Yin K. A review of process fault detection and diagnosis. Part III: process history based methods. *Comput Chem Eng*. 2003;27:327–346.
4. Yoon S, MacGregor JF. Statistical and causal model-based approaches to fault detection and isolation. *AIChE J*. 2000;46:1813–1824.
5. Jackson JE. *A User's Guide to Principal Components*. New York: Wiley, 1991.
6. Kourti T, MacGregor JF. Multivariate SPC methods for process and product monitoring. *J Qual Technol*. 1996;28:409–428.
7. Westerhuis JA, Gurden SP, Smilde AK. Generalized contribution plots in multivariate statistical process monitoring. *Chemom Intell Lab Syst*. 2000;51:95–114.
8. Höskuldsson A. PLS regression methods. *J Chemom*. 1988;2:211–228.
9. MacGregor JF, Jaeckle C, Kiparissides C, Koutoudi M. Process monitoring and diagnosis by multiblock PLS methods. *AIChE J*. 1994;40:826–838.
10. Kourti T, MacGregor JF. Process analysis, monitoring and diagnosis, using multivariate projection methods. *Chemom Intell Lab Syst*. 1995;28:3–21.
11. Russell EL, Chiang LH, Braatz RD. Fault detection in industrial processes using canonical variate analysis and dynamic principal component analysis. *Chemom Intell Lab Syst*. 2000;51:81–93.
12. Ku W, Storer RH, Georgakis C. Disturbance detection and isolation by dynamic principal component analysis. *Chemom Intell Lab Syst*. 1995;30:179–196.
13. Martin EB, Morris AJ. Non-parametric confidence bounds for process performance monitoring charts. *J Process Control*. 1996;6:349–358.
14. Silverman BW. *Density Estimation for Statistics and Data Analysis*. London: Chapman & Hall, 1986.
15. Chen Q, Kruger U, Leung AYT. Regularised kernel density estimation for clustered process data. *Control Eng Pract*. 2004;12:267–274.
16. Chen Q, Kruger U, Meronk M, Leung AYT. Synthesis of T^2 and Q statistics for process monitoring. *Control Eng Pract*. 2004;12:745–755.
17. Theodoridis S, Koutroumbas K. *Pattern Recognition*. San Diego: Academic Press, 1999.
18. Banerjee A, Arkun Y, Ogunnaike B, Pearson R. Estimation of nonlinear systems using linear multiple models. *AIChE J*. 1997;43:1204–1226.
19. Deshpande AP, Patwardhan SC. Online fault diagnosis in nonlinear systems using the multiple operating regime approach. *Ind Eng Chem Res*. 2008;47:6711–6726.
20. Wang XZ, McGreavy C. Automatic classification for mining process operational data. *Ind Eng Chem Res*. 1998;37:2215–2222.
21. Yu J, Qin SJ. Multimode process monitoring with Bayesian inference-based finite Gaussian mixture models. *AIChE J*. 2008;54:1811–1829.
22. Mehranbod N, Soroush M, Piovoso M, Ogunnaike BA. Probabilistic model for sensor fault detection and identification. *AIChE J*. 2003;49:1787–1802.
23. Mehranbod N, Soroush M, Panjapornpon C. A method of sensor fault detection and identification. *J Process Control*. 2005;15:321–339.
24. Kruger U, Dimitriadis G. Diagnosis of process faults in chemical systems using a local partial least squares approach. *AIChE J*. 2008;54:2581–2596.
25. Krugera U, Kumarb S, Littlera T. Improved principal component monitoring using the local approach. *Automatica*. 2007;43:1532–1542.
26. Raich A, Çinar A. Statistical process monitoring and disturbance duagnosis in multivariable continuous processes. *AIChE J*. 1996;42:995–1009.
27. Raich A, Çinar A. Diagnosis of process disturbances by statistical distance and angle measure. *Comput Chem Eng*. 1997;6:661–673.
28. He QP, Qin SJ, Wang J. A new fault diagnosis method using fault directions in Fisher discriminant analysis. *AIChE J*. 2005;51:555–571.
29. Liu J, Chen DS. Fault detection and identification using modified Bayesian classification on PCA subspace. *Ind Eng Chem Res*. 2009;48:3059–3077.
30. Berhouex PM, Box GE. Time series models for forecasting wastewater treatment plant performance. *Water Res*. 1996;30:1865–1875.
31. Chen Q, Kruger U, Leung AYT. Cointegration testing method for monitoring nonstationary processes. *Ind Eng Chem Res*. 2009;48:3533–3543.
32. Dempster AP, Laird NM, Rubin DB. Maximum-likelihood from incomplete data via the EM algorithm. *J R Stat Soc Ser B*. 1977;39:1–38.
33. McLachlan G, Peel D. *Finite Mixture Models*. New York: Wiley, 2000.
34. Conlin AK, Martin EB, Morris AJ. Confidence limits for contribution plots. *J Chemom*. 2000;14:725–736.
35. Johansson KH. The quadruple-tank process: a multivariable laboratory process with an adjustable zero. *IEEE Trans Control Syst Technol*. 2000;8:456–465.

Manuscript received Feb. 12, 2009, and revision received May 31, 2009.